Early effects of Aβ1-42 oligomers injection in mice: Involvement of PI3K/Akt/GSK3 and MAPK/ERK1/2 pathways

Research report

Early effects of Aβ1-42 oligomers injection in mice: Involvement of I3K/Akt/GSK3 and MAPK/ERK1/2 pathways

Fabiana Morroni[a,*,1], Giulia Sita[a,1], Andrea Tarozzi[b], Roberto Rimondini[c], Patrizia Hrelia[a]

[a] Department of Pharmacy and Biotechnology, Alma Mater Studiorum—University of Bologna, via Irnerio 48, 40126 Bologna, Italy
[b] Department for Life Quality Studies, Alma Mater Studiorum—University of Bologna, Corso d'Augusto, 237, 47900 Rimini, Italy
[c] Department of Medical and Clinical Sciences, Alma Mater Studiorum—University of Bologna, via Irnerio 48, 40126 Bologna, Italy

highlights

- Aβ oligomers (AβO) injection induces learning and memory impairments
- AβO injection increases oxidative stress and GSH levels
- AβO injection induces caspase-9 activation
- AβO injection decreases immunofluorescence reactivity of synaptophysin
- AβO toxicity leads to the activation of Akt and ERK1/2, and decreases GSK3 activity

Keywords:
Beta-amyloid
Cognitive impairment
Oxidative stress
Akt
ERK1/2
GSK3

abstract

Neuronal and synaptic loss are the best pathological correlates for memory decline in Alzheimer's disease (AD) Soluble beta-amyloid oligomers (AβO) are considered to putatively play a crucial role in the early synapse loss and cognitive impairment observed in AD Evidence suggests that oxidative stress and apoptosis are involved in the mechanism of Aβ-induced neurotoxicity and AD pathogenesis This study aimed to explore the molecular mechanisms that contribute to the early memory deficits induced by intracerebroventricular injection of AβO in mice Ten days after a single AβO injection memory impairments were observed, as measured by Morris water maze and novel object recognition tests Cognitive decline was associated with increased oxidative stress, caspase-9 activation, and decreased hippocampal synaptophysin immunoreactivity Furthermore, GSH levels were significantly higher in AβO-injected mice than in sham mice, showing that a protective mechanism might develop due to oxidative stress Additionally, AβO-induced toxicity was aligned with an increment of the activation of Akt and ERK1/2, and reduced activity of GSK3 These findings suggest that AβO injection triggers a cascade of events that mimic the key neuropathological hallmarks of AD Aβ acute injection helps to better understand how this peptide impairs specific signaling pathways leading to synaptic and memory dysfunctions Thus, this model is a valid tool for investigating AD and may suggest a new way to develop neuroprotective therapies at such early stages of the disease

1. Introduction

Alzheimer's disease (AD) is the most common cause of progressive cognitive impairment in the aging population. The scenario is worrying: disease-modifying therapies are still not available, and existing strategies do not target potential causes of AD but rather downstream events in the disease. The accumulation of senile plaques and neurofibrillary tangles are widely accepted as neuropathological hallmarks of the AD brain. They are associated with neuronal loss and synaptic dysfunction which lead to the progressive impairments in learning and memory. Currently, the "Aβ hypothesis" [1] is commonly accepted as playing a crucial role in the pathogenesis of AD in which amyloid beta peptide (Aβ), the main component of senile plaques, orchestrates the development of AD.

* Corresponding author at: Department of Pharmacy and Biotechnology, via Irnerio 48, 40126 Bologna, Italy
E-mail address: fabiana morroni@unibo it (F Morroni)
[1] These authors contributed equally to this work

A growing number of studies have shown that soluble oligomeric forms are more neurotoxic than amyloid fibrils, especially in synaptic transmission, and closely involved in AD progression [2,3]. It was demonstrated that the level of Aβ oligomers (AβO) is increased in AD brains and correlates with disease severity [4]. Although several isoforms exist, ranging in length from 39 to 43 residues, $Aβ_{1-40}$ and $Aβ_{1-42}$ are the most physiologically relevant. In AD patients, $Aβ_{1-40}$ is the most abundant, but $Aβ_{1-42}$ has the ability to form the core of Aβ plaque deposition prior to aggregation [5]. However, the exact mechanism by which Aβ causes neuronal toxicity and cognitive impairment is not yet clearly understood.

Injection of $Aβ_{1-42}$ mimics the amyloid toxicity and endogenous accumulation observed in AD physiopathology. It has been suggested that $Aβ_{1-42}$ injection could serve as a useful animal model of AD [6,7]. This model could help to understand the molecular detail of how AD develops, thus representing a crucial step towards determining which molecules and pathways should be targeted to efficiently halt or prevent neurological outcomes. AD is primarily a sporadic disorder: age is the main risk factor [8] and fewer than 5% of cases appear associated with familial inheritance [9]. Thus, the identification of toxins that accumulate with aging in the AD brain and the aberrant signaling pathways that lead to synapse dysfunction is undoubtedly essential to pave the way for successful new therapeutic approaches.

Increasing evidence has indicated that AD is characterized by a heightened oxidative environment in the brain and subsequent neurodegeneration. The accumulation of Aβ seems to increase oxidative stress and lead to mitochondrial dysfunction and energy failure even in the early stage of AD [10]. In addition to the accumulation of free radical species, alterations in the activities or expression of antioxidant enzymes have been observed in both the central nervous system and peripheral tissues of AD patients [11,12]. Moreover, in AD and mild cognitive impairment (MCI) brains, the increased oxidative damage and the decline of glutathione (GSH) and antioxidant enzyme activities are more localized in the synapses and correlate with the severity of the disease, suggesting an involvement of oxidative stress in AD-related synaptic loss [13].

It is widely accepted that apoptosis takes place in the pathogenesis of AD [14]. Researchers have found that the brains of AD patients contain dying neurons that display some characteristic signs of apoptosis such as DNA fragmentation and activation of caspases that carry out the death program [15]. Despite the significant improvement in research related to apoptotic mechanisms there is no substantial therapeutic strategy to stop or slow this process. In neurons, the ERK pathway and the PI3K/AKT pathway are important mediators of cell growth, survival and differentiation [16], and there is crosstalk between the two signaling pathways. Moreover, GSK-3β is a pleiotropic enzyme involved in a variety of cell activities, and has been postulated as a therapeutic target for AD due to its multiple connections to the pathology of the disease [17]. However, the mechanisms involved in the activation/inhibition of these pathways and the way in which they interact to execute cell death remain poorly understood.

Here, we focus on the discovery of soluble Aβ oligomers (AβO) as toxins that accumulate in the AD brain and target synapses, and how these findings have led to significant advances in our understanding of mechanisms of memory impairment. Our model of local administration of Aβ peptide into the mice brain represents a model of early AD. In this study, we examined the effects of AβO on learning and memory, redox status, GSH levels, caspase activity and synaptic function. To further investigate a possible molecular mechanism underlying AβO toxicity, we determined the levels of Akt, ERK1/2 and phosphorylated GSK-3.

2. Material and methods

2.1. Animals

Male C57Bl/6 (9 weeks old, 25–30 g body weight at the beginning of the experiment; Harlan, Milan, Italy) mice were housed under 12 h light/12 h dark cycle (lights on from 7:00 a.m. to 7:00 p.m.) with free access to food and water in a temperature- and humidity-controlled room. Briefly, all experiments were carried out in accordance with Directive 2010/63/EU and approved by the corresponding committee at the University of Bologna (PROT. n. IX/77 2013). Care was taken to minimize the number of experimental animals and to take measures to limit their suffering. Mice were allowed to acclimatize for at least 1 week before the start of experiments. Animals were randomly assigned to two groups (n = 10/group) as follows: Aβ and sham. One group received an intracerebroventricular (i.c.v.) injection of $Aβ_{1-42}O$, while the other group received the same volume of saline. At 10 days post injection, mice were tested for Morris Water Maze (MWM) and Novel Object Recognition (NOR) tests. After the behavioral assessment, mice were sacrificed by cervical dislocation to perform immunohistochemistry and neurochemical analysis.

2.2. Aβ oligomer preparation and injection

$Aβ_{1-42}$ peptides (AnaSpec, Fremont, CA, USA) were first dissolved in hexafluoroisopropanol to 1 mg/mL, sonicated, incubated at room temperature for 24 h and lyophilized. The resulting unaggregated $Aβ_{1-42}$ film was dissolved with sterile dimethylsulfoxide and stored at −20 °C until use. The $Aβ_{1-42}$ aggregation to oligomeric form was prepared as described previously by Tarozzi et al. [18]. Briefly, $Aβ_{1-42}$ stock in DMSO was diluted into phosphate buffer saline (PBS) at 40 μM and incubated at 4 °C for 48 h to enhance oligomer formation [19] and [20]. To analyze the morphology of aggregated $Aβ_{1-42}$ forms, transmission electron microscopy was used as previously reported [21]. Aggregated $Aβ_{1-42}$ solution was absorbed onto formvar-carbon coated grids (200 mesh size) for 40 min and stained with 2% aqueous phosphotungstic acid solution before viewing with a Philips CM10 transmission electron microscope at 80 kV.

Six μL of $Aβ_{1-42}O$ (40 μM) were injected i.c.v. under gaseous anesthesia (2% isoflurane in 1L/min oxygen/nitrous oxide), using a stereotaxic mouse frame (myNeuroLab, Leica-Microsystems Co, St. Louis, MO, USA) and a 10 μL Hamilton syringe, at a rate of 0.5 mL/min. The needle was left in place for 3 min after the injection before slow retraction, followed by cleaning and suturing of the wound. Sham mice received the equivalent volume of saline into the ventricle. The injection was performed at the following coordinates: AP: + 0.22, ML: + 1.0, DV: − 2.5, with a flat skull position.

2.3. Behavioral analysis

All tests were carried out between 9.30 a.m. and 3.30 p.m. Animals were transferred to the experimental room at least 1 h before the test in order to let them acclimatize to the test environment. All scores were assigned by the same observer who was unaware of the animal treatment.

2.3.1. Morris water maze (MWM) test

The apparatus used for the MWM task was a circular plastic tank (1.0 m diameter, 50 cm height) filled with water and milk maintained at 22° C. The maze was located in a room containing several simple visual, extra-maze cues that were constant throughout the study. A transparent platform was set inside the tank and its top was submerged 1.5 cm below the water surface in the center of one among the four quadrants of the maze. The movements of

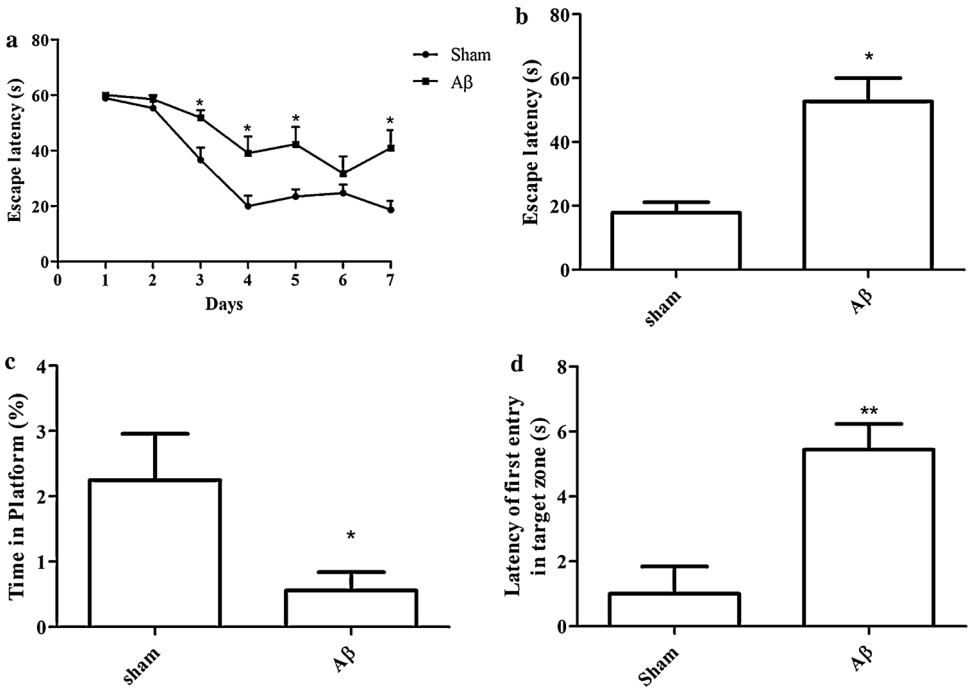

Fig. 1. Effects of $A\beta_{1\text{-}42}O$ injection on the performance of mice in the training (a) and probe trial (b–d) of the Morris Water Maze test The training trials were carried out for 7 days (four per day), the probe trials were performed on day 8 Escape latency (b), time spent in target zone (c) and latency of first entry in target zone (d) in the 24 h probe test Values are expressed as mean ± SEM ($n = 10$) (a–c: *p < 0 05 vs sham group, d: **p < 0 01 vs sham group; *t*-test)

the animal in the tank were monitored with a video tracking system (EthoVision, Noldus, The Netherlands). For each training trial, the mouse was put into the pool at one of the four positions, the sequence of the positions being selected randomly. The platform was located in a constant position throughout the test period in the middle of one quadrant. In each training session, the latency to escape on the hidden platform was recorded. If a mouse failed to find the platform within 60 s, it was manually guided to the platform and allowed to remain there for 10 s. After the trial, each mouse was placed into a holding cage under a warming lamp for 25 s until the start of the next trial. Training was conducted for 7 days, four times a day. Ninety min and 24 h after the last training session probe trials were performed, consisting of a 60 s free swim in the pool without the platform. The parameters measured during the probe trial included escape latency, time spent in the target zone, and latency of first entry in the target zone.

2.3.2. *Novel object recognition (NOR) test*

This task is based on the spontaneous tendency of rodents to explore novel objects [22]. The test was performed in an apparatus made of a white Plexiglas box (60 60 30 cm) with the floor divided into four identical squares in a dim room. Mice were placed in the empty box for 5 min 24 h prior to exposure to objects, in order to habituate them to the apparatus and test room. Twenty-four hours after habituation, mice were acclimated in the test room for 1 h before the beginning of the sessions. Firstly, mice completed an acquisition trial (24 h after habituation) that consisted of leaving the animals in the apparatus containing two identical objects (A and A'). After a 90 min retention interval, the mice were placed back into the arena and exposed to the familiar object (A) and to a novel object (B) for short-term recognition memory test. Twenty four h later, long-term recognition memory was evaluated and a different pair of dissimilar objects (a familiar and a novel one; A and C, respectively) were presented. In all sessions, each mouse was always placed in the apparatus facing the wall and allowed to explore the objects for 5 min, after which the mouse was returned to its home cage. Behavior was recorded by a video camera mounted vertically above the test arena and analyzed using appropriated video-tracking software (EthoVision, Noldus). Between trials, the apparatus was cleaned with 5% ethanol solution to eliminate animal clues. The light inside the apparatus was maintained at a minimum to avoid any anxiety behavior. A recognition index, a ratio of the amount of time spent exploring the novel object over the total time spent exploring both objects, was used to measure cognitive function.

2.4. *Tissue preparation for immunohistochemistry and neurochemical analysis*

Once behavioral analysis was completed, mice were deeply anesthetized and sacrificed by cervical dislocation. The brains were removed and the left hemisphere of each animal was immersed in a 4% fixative solution of paraformaldehyde (Santa Cruz Biotechnology, Dallas, TX, USA) for 48 h. Right hemispheres were rapidly removed, and the cerebral cortex and the hippocampus were dissected in an ice-cold plastic dish. Samples were then snap frozen in liquid nitrogen, and kept at −80 °C until analysis. Tissues were homogenized in lysis buffer (50 mM Tris, pH 7.5, 0.4% NP-40, 10% glycerol, 150 mM NaCl, 10 μg/mL aprotinin, 20 μg/mL leupeptin, 10 mM EDTA, 1 mM sodium orthovanadate, 100 mM sodiumfluoride), and protein concentration was determined by the Bradford method.

2.5. *Determination of redox status*

The redox status, in terms of reactive oxygen species (ROS) formation, was measured as described previously [23], based on the oxidation of 2 7 -dichlorodihydrofluorescein diacetate (DCFH-DA) to 2 7 -dichlorofluorescein (DCF). Briefly, the reaction mixture (60 μL) containing 2 mg/mL of DCFH-DA was incubated for 30 min to allow the DCFH-DA to be incorporated into any membrane-bound vesicles and the diacetate group to be cleaved by esterases.

After 30 min of incubation, the conversion of DCFH-DA to the fluorescent product DCF was measured using a microplate reader (GENios, TECAN®) with excitation at 485 nm and emission at 535 nm. Background fluorescence (conversion of DCFH-DA in the absence of homogenate) was corrected by the inclusion of parallel blanks. Values were normalized to protein content and expressed as the mean of fluorescence intensity arbitrary units (UF) of each experimental group.

2.6. Determination of glutathione (GSH) content

GSH content was assessed using the protocol described earlier [24]. Briefly, aliquots of 50 μL of samples were precipitated with 100 μL of sulfosalicylic acid (4%). The samples were kept at 4 °C for at least 1 h and then subjected to centrifugation at 3000 rpm for 10 min at 4 °C. A volume of 25 μL of the assay mixture and 50 μL of 5-5 -dithiobis (2-nitrobenzoic acid) (4 mg/mL in phosphate buffer, 0.1 M, pH 7.4) was made up to a total volume of 500 μL. The yellow color that developed was read immediately at 412 nm (GENios, TECAN®) and results were calculated using a standard calibration curve. Values are expressed as GSH mmol/mg of total lysate proteins per assay.

2.7. Determination of caspase-9 activation

Caspase-9 enzyme activity was determined using a protocol adapted by Movsesyan et al. [25]. The assay is based on the hydrolysis of the *p*-nitroaniline (pNA) moiety by caspase-9. Briefly, tissue lysates were incubated with assay buffer (50 mmol/L Hepes, pH 7.4; 0.2% CHAPS; 20% sucrose; 2 mmol/L EDTA; and 10 mmol/L dithiothreitol) and a 50 mmol/L concentration of chromogenic pNA specific substrate (Ac–Leu–Glu–His–Asp–pNA; Alexis Biochemicals, San Diego, CA, USA). In a final volume of 100 μL (containing 60 μg of protein), each test sample was incubated for 3 h at 37 °C. The amount of chromogenic pNA released was measured with a microplate reader (GENios, TECAN®) at 405 nm. Values are expressed as the mean of optical density (OD) of each experimental group.

2.8. Western blotting

Samples (30 μg proteins) were separated on 12% SDS polyacrylamide gels (Bio-Rad, Hercules, CA, USA) and electroblotted onto 0.2 μm nitrocellulose membranes. Membranes were incubated overnight at 4 °C with primary antibody recognizing Phospho-p44/42 MAPK (Erk1/2) (Thr202/Tyr204), Phospho-Akt (Ser473) or Phospho-GSK-3 /β (Ser21/9) (1:1000; Cell Signaling Technology Inc., Danvers, MA, USA). Membranes were washed with TBS-T (TBS +0.05% Tween20), and then incubated with a horseradish peroxidase (POD) linked anti-rabbit secondary antibody (1:2000; GE Healthcare, Piscataway, NJ, USA). Immunoreactive bands were visualized by enhanced chemiluminescence (ECL; Pierce, Rockford, IL, USA). The same membranes were stripped and reprobed with total p44/42 MAPK (1:1000; Cell Signaling Technology Inc.), total Akt (1:1000; Cell Signaling Technology Inc.), or total GSK-3 /β (1:1000; Cell Signaling Technology Inc.). Data were analyzed by densitometry, using Quantity One software (Bio-Rad). Values were normalized to corresponding p44/42 MAPK, Akt or GSK3 and expressed as fold increase.

2.9. Immunohistochemistry

2.9.1. Caspase-9 staining

Fixed brains were sliced on a vibratome (Leika Microsystems, Milan, Italy) at 40 μm thickness. After deparaffinization, endogenous peroxidase was quenched with 3% hydrogen peroxide (H_2O_2). Non-specific adsorption was minimized by incubating the section in 10% normal goat serum for 30 min. Sections were then incubated overnight, at 4 °C, with a rabbit anti-cleaved caspase-9 (1:500; Cell Signaling Technology Inc.), rinsed in TBS, and re-incubated for 1 h, at room temperature, with a goat biotinylated anti-rabbit IgG antibody (Vector Laboratories, Burlingame, CA, USA). Finally, sections were processed with the avidin-biotin technique and reaction products were developed using commercial kits (Vector Laboratories). To verify the binding specificity, some sections were also incubated with only primary antibody (no secondary) or with the secondary antibody (no primary). In these situations, no positive staining was found in the sections, indicating that the immunoreactions were positive in all experiments carried out.

2.9.2. Synaptophysin staining

Fixed brains were sliced on a vibratome (Leika Microsystems) at 40 μm thickness. After deparaffinization, permeabilization was obtained by 0.1% Triton X-100 solution (Sigma Aldrich, Saint Louis, MO, USA). Non-specific adsorption was minimized by incubating the section in 2% albumin (Sigma Aldrich) for 30 min. Sections were then incubated overnight at 4 °C with a mouse monoclonal anti-synaptophysin antibody (1: 500; Sigma Aldrich), rinsed in TBS, and re-incubated for 1 h, at room temperature, with a goat anti-mouse Alexa Fluor® 488 (1: 200; Life Technologies, Monza, MB, Italy). To verify the binding specificity, some sections were also incubated with only primary antibody (no secondary) or with the secondary antibody (no primary). In these situations, no positive staining was found in the sections, indicating that the immunoreactions were positive in all experiments carried out.

2.9.3. Quantitative image analysis

Image analysis was performed by a blinded investigator, using an AxioImager M1 microscope (CarlZeiss, Oberkochen, Germany) and a computerized image analysis system (AxioCam MRc5, Zeiss) equipped with dedicated software (AxioVision Rel 4.8, Zeiss). After defining the boundary of the hippocampus at low magnification (2.5 ×objective), capase-9 activation or synaptic function were evaluated by densitometry of five different sections for each sample analyzed at a higher magnification (40× objective). Quantification and morphological analysis were performed with the ImageJ software.

2.10. Statistical analysis

Data were analyzed with the PRISM 5 software (GraphPad Software, La Jolla, CA, USA) and expressed as the mean±SEM of each group. The difference between groups was analyzed with a two-tailed *t*-test. A difference was considered statistically significant when a p value was less than 0.05.

3. Results

3.1. Effect of A˜$_{1-42}$ on the performance in the MWM test

To investigate the effects of Aβ_{1-42}O on spatial learning and memory in mice, the MWM test was performed. Escape latency reductions from day to day reflected learning with respect to long-term memory. According to the results, i.c.v. injection of Aβ_{1-42}O after 10 days could impair the learning ability of animals and this was shown by the increased escape latency during training days (Fig. 1a). The results of the 24 h probe test are presented in Fig. 1b–d (90 min probe test, see Supplementary Fig. S1). The Aβ-injected group spent less time in the platform zone ($p < 0.05$) and the escape latency remarkably increased ($p < 0.05$) both in short- and long-term evaluation, demonstrating memory impairment in this group compared to the sham group. No alterations in swimming speed

and total distance travelled were observed (data not shown), indicating there were no motor deficits in this animal model.

3.2. Effect of A˘1-42on the performance in the NOR test

A recognition index (RI), which is the percentage of time spent exploring the new object over the total time spent exploring the two objects, was determined. An RI of 50% is equivalent to the chance level, and a higher RI in the test phase indicates preferable object recognition memory. In the training phase, the mice of both groups spent a comparable time exploring the two objects (data not shown). The sham group could discriminate the novel object from the familiar object if tested 1 day after training, with the RI (68.4%) being significantly higher than the 50% chance level, but the mice Alϑ1–42O injected 10 days before the training phase failed to distinguish the novel object from the familiar object, and the average RI of this group (51.1%) was significantly lower than the control value (Fig. 2, $p < 0.05$). The short term evaluation (90 min) did not show any significant differences (see Supplementary Fig. S2).

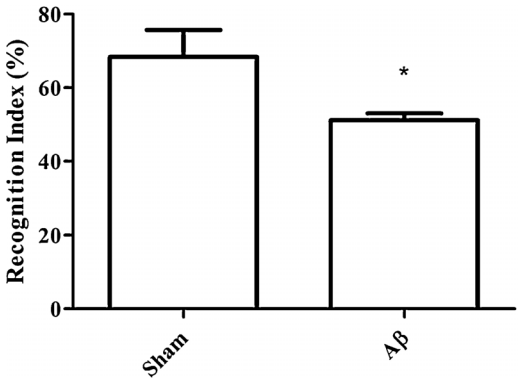

Fig. 2. Effects of Alϑ1-42 O injection on the performance of mice in the Novel Object Recognition test Quantitative comparison of the recognition index in memory test session, which was performed 24 h after the training session Values are expressed as mean ± SEM ($n = 10$) (*p < 0 05 vs sham group; *t*-test)

3.3. Effect of A˘1-42on redox status and GSH level in the hippocampus and cerebral cortex

Increasing evidence shows that Alϑ1–42 can induce mitochondrial dysfunction followed by the overproduction of ROS. As an index of redox status, we utilized the fluorescent probe DCFH-DA to measure ROS levels in cortical and hippocampal tissues of the mice. This showed that, compared with the sham group, ROS levels in the hippocampus (Fig. 3a) and cerebral cortex (Fig. 3b) of Alϑ1-42 injected mice were significantly increased ($p < 0.05$).

GSH is a vital extracellular and intracellular protective antioxidant against oxidative stress. It reduces hydrogen peroxides and hydroperoxides by redox and detoxification reactions as well as protects protein thiol groups from oxidation. GSH has been shown to be essential against various oxidative stressors found in AD [17]. We evaluated the level of GSH in the hippocampus and cerebral cortex to elucidate whether Alϑ1–42O injection could make any change in the antioxidant status within the brain. As shown in Figs. 3c and d, the level of GSH was significantly higher in the Alϑ treated mice than in the sham group ($p < 0.001$).

3.4. Effect of A˘1-42on caspase-9 activation in the hippocampus and cerebral cortex

Caspase-9 is a known biomarker of oxidative stress-induced cell death which is mediated via the mitochondria-dependent apoptotic pathway. To determine whether Alϑ1–42O increases neuronal apoptosis in mice hippocampus and cerebral cortex, we determined

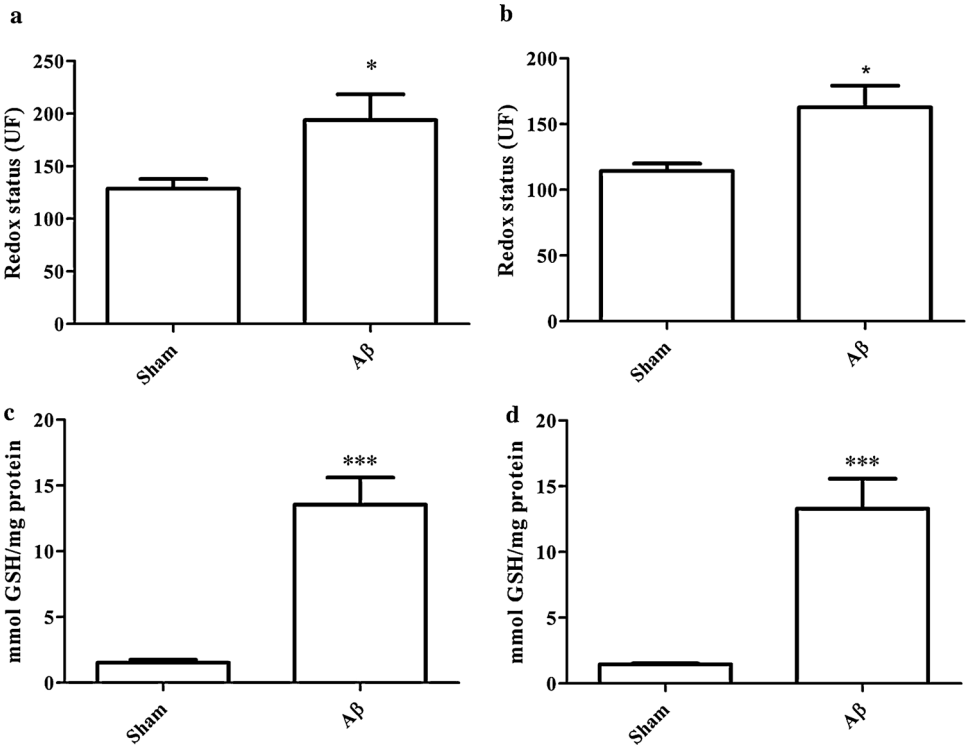

Fig. 3. Effects of Alϑ1-42 O injection on redox status and GSH content Redox status was determined in the hippocampus (a) and cerebral cortex (b) based on DCF's fluorescence emission at 535 nm after excitation at 485 nm Values are expressed as mean ± SEM (n = 10) of fluorescence intensity arbitrary units (UF) of each experimental group GSH content was measured using a colorimetric assay in the hippocampus (c) and cerebral cortex (d) Values are calculated using a standard calibration curve and expressed as mmol GSH/mg protein (a, b: *p < 0 05 vs sham group,; c, d: ***p < 0 001 vs sham group; *t*-test)

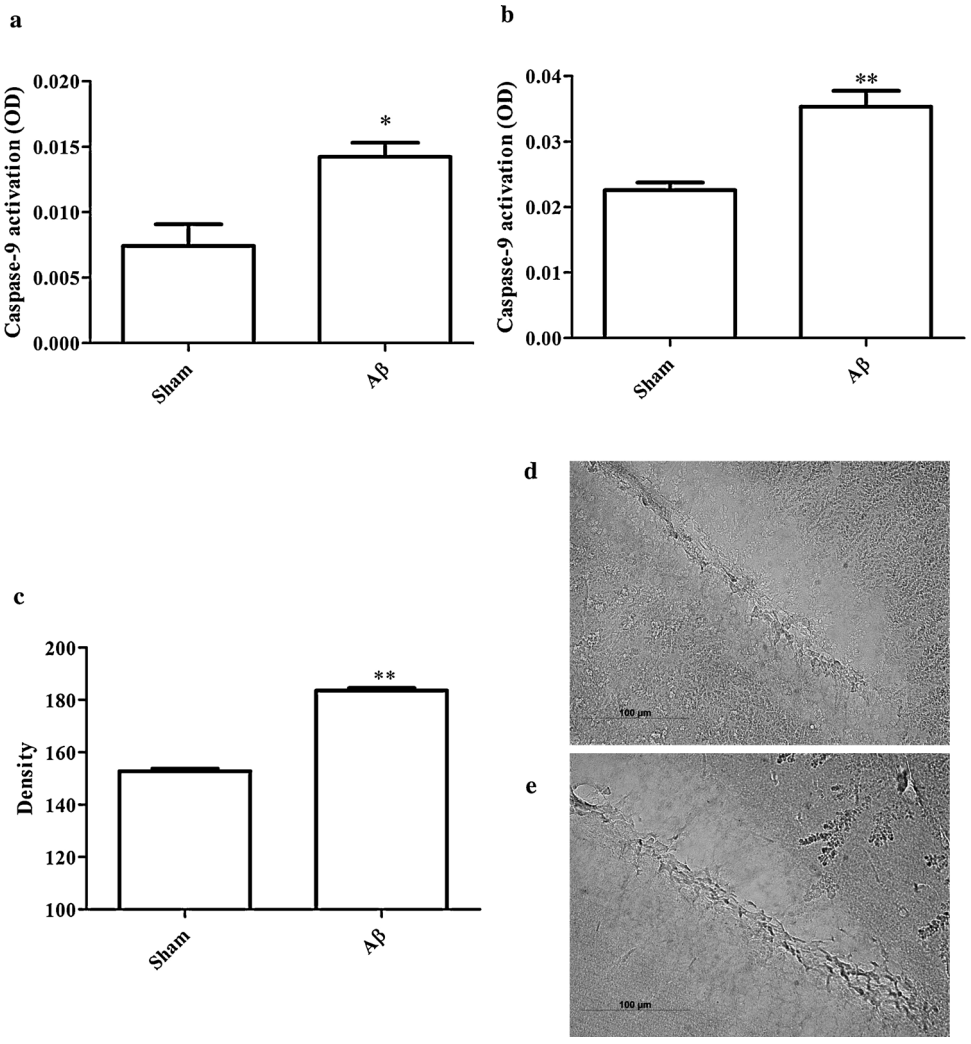

Fig. 4. Effects of $Ab_{1-42}O$ injection on caspase-9 activation Caspase-9 activity was determined using specific chromogenic substrate in the hippocampus (a) and cerebral cortex (b) Values are expressed as mean ± SEM (n = 10) of optical density (OD) of each experimental group (a: *p < 0 05 vs sham group; b: **p < 0 01 vs sham group; t-test) Caspase-9 immunoreactivity was performed in hippocampal sections Quantitative analysis of caspase-9 immunostaining (c) Representative photomicrographs of immunostaining for cleaved caspase-9 in brain coronal sections containing hippocampal structure of sham (d) and Aβ (e) mice Scale bar 100 μm Values are expressed as mean ± SEM (n = 10) of the density of each experimental group (c: **p < 0 01 vs sham group; t-test)

caspase-9 activation using a colorimetric method. Our data showed that $A\beta_{1-42}O$-injection resulted in activation of caspase-9 (Fig. 4a and b) both in the hippocampus ($p < 0.05$) and cerebral cortex ($p < 0.01$). We also examined the possible activation of caspase-9 in the mouse brain using an antibody that recognizes the active fragments of caspase-9. In vivo immunohistochemical analysis demonstrated significant caspase-9 activation in the majority of hippocampal brain sections from control brains (Fig. 4c–e, $p < 0.01$).

3.5. *Effect of Aβ_{1-42} on ERK1/2, Akt and GSK3 phosphorylation in the hippocampus and cerebral cortex*

Some studies have proposed that Akt and ERK are involved in Aβ toxicity both in animal models [26] and hippocampal slices [27]. Among the mitogen-activated kinase (MAPK) family, a role for the ERK1/2 signaling pathway in neuronal death has been proposed [28]. To explore the effects of $A\beta_{1-42}O$ on ERK1/2 activity, the amount of its phosphorylation was assessed by western blot studies. In our experimental model, $A\beta_{1-42}O$ induced a significant increase of ERK1/2 activity both in hippocampal and cerebral cortex samples ($p < 0.05$, Fig. 5a and b).

Akt is a serine-threonine kinase that, among its targets, has GSK3, a kinase constitutively active in cells and inhibited through phosphorylation by Akt. Interestingly, both in the hippocampus and cerebral cortex, $A\beta_{1-42}O$ exhibited a significant activation of Akt ($p < 0.05$, Fig. 5c and d). As shown in Fig. 5e and f, the increase of GSK3 phosphorylation on Ser9, which corresponds to its inactivity, was similar to that observed for Akt ($p < 0.05$).

3.6. *Effect of Aβ_{1-42} on synaptic functions*

Compelling evidence indicates that Aβ, especially the soluble oligomers, selectively targets synapses and disrupts their structures and functions [29]. To analyze the effect of $A\beta_{1-42}O$ on synaptic function, we assessed the expression of the presynaptic protein synaptophysin. Immunofluorescence results showed decreased immunofluorescence reactivity of synaptophysin in the hippocampus of $A\beta_{1-42}$-treated mice as compared to the sham group ($p < 0.001$, Fig. 6).

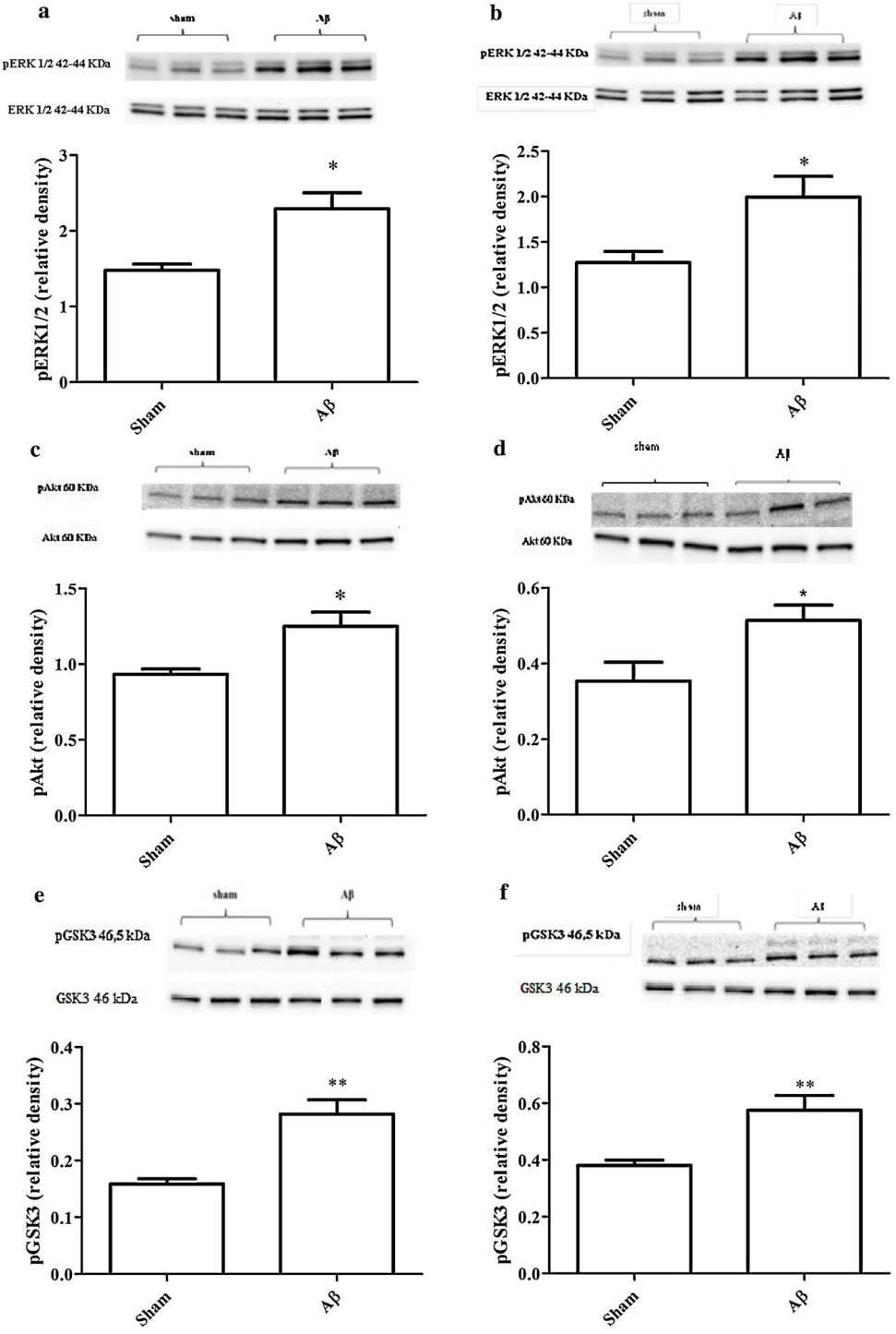

Fig. 5. Effects of $A\beta_{1\text{-}42}O$ injection on ERK1/2, Akt and GSK3 phosphorylation Western immunoblots probed with antibodies against pERK1/2 and ERK1/2 (a, b) Top: representative images of protein expression in the hippocampus (a) and cerebral cortex (b) Bottom: quantitative analysis of the Western Blot results for the pERK1/2 levels in the hippocampus (a) and cerebral cortex (b) Western immunoblots probed with antibodies against pAkt and Akt (c, d) Top: representative images of protein expression in the hippocampus (c) and cerebral cortex (d) Bottom: quantitative analysis of the Western Blot results for the pAkt levels in the hippocampus (c) and cerebral cortex (d) Western immunoblots probed with antibodies against pGSK3 and GSK3 (e, f) Top: representative images of protein expression in the hippocampus (e) and cerebral cortex (f) Bottom: quantitative analysis of the Western Blot results for the pGSK3 levels in the hippocampus (e) and cerebral cortex (f) Values are expressed as mean of fold increase ± SEM ($n = 10$) (a–d:*p < 0 05, e,f:**p < 0 01 vs sham group; *t*-test)

4. Discussion

According to our current knowledge, there is still no animal model with all the cognitive, behavioral, biochemical and histopathological abnormalities that characterize AD. The published studies have demonstrated that i.c.v. injection with $A\beta_{1-42}$ to mice could induce significant neuron death, inflammatory response and memory impairments [6,30]. In this study, mice treated with $A\beta_{1-42}$ oligomers showed longer escape latency and shorter swimming time in the target quadrant (MWM test) and lower recognition memory (NOR test) compared with sham group. Moreover, we found that ROS formation and the levels of GSH increased con-

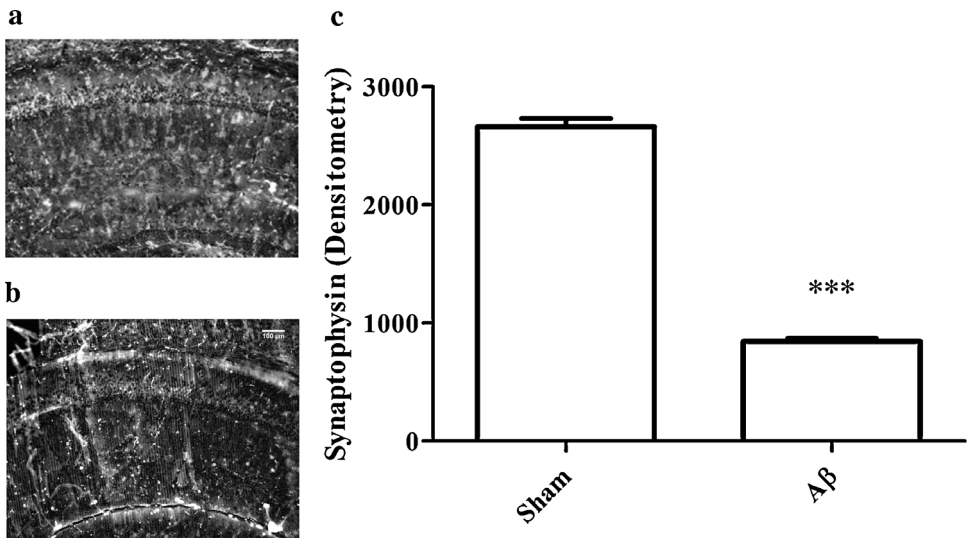

Fig. 6. Effects of $Ab_{1-42}O$ injection on synaptic functions (a, b) Representative photomicrographs of immunostaining for synaptophysin in brain coronal sections containing hippocampal structure of sham (a) and Aβ (b) mice Scale bar 100 μm Quantitative analysis of synaptophysin immunostaining (c) Values are expressed as mean ± SEM ($n = 10$) of the fluorescent intensity of each experimental group (c: ***$p < 0\ 001$ vs sham group; *t*-test)

siderably within the cerebral cortex and hippocampus, indicating that $A\beta_{1-42}O$ could generate oxidative stress in mice brain. At the same time, $A\beta_{1-42}O$ triggered the activation of caspase-9 in the hippocampus and cerebral cortex, which eventually resulted in neuronal apoptosis, and impaired synaptic function. In summary, $A\beta_{1-42}$ partially simulated the earlier stage characteristics of learning and memory obstacles of AD.

Alterations of GSH levels have been observed in various neurodegenerative processes and GSH depletion is usually associated with neurotoxicity in animal models. This study showed that GSH levels increased significantly in the hippocampus and cerebral cortex after $A\beta_{1-42}O$ injection in mice. This result is thought to explain a compensatory rise in the GSH-related antioxidant system in response to increased ROS formation. Our findings are supported by Cetin and Dincer [31], who have shown that increased levels of GSH in temporal cortex and basal forebrain after intrahippocampal $A\beta_{1-42}$ injection could be a protective mechanism due to oxidative stress.

One of the most obvious consequences of oxidative stress-induced DNA damage is cell apoptosis by inducing mitochondrial permeability transition pore [32]. The mitochondrial transition pore is considered the "point of no return" for apoptotic cell death, which is able to switch cells to apoptotic death via oxidative stress-responsive signaling cascades [33]. The involvement of the apoptotic pathway in the toxicity of $A\beta_{1-42}O$ was already described in our in vitro models [34,35]. In particular, the activation of procaspase-9 is the triggering event of the mitochondrial apoptotic pathway. In our model, 10 days after $A\beta_{1-42}$ injection caspase-9 was significantly activated; this activation coexists with memory defect and synaptic dysfunction (as shown by synaptophysin decreased immunofluorescence) and might direct us to the conclusion that $A\beta_{1-42}O$-induced apoptosis leads to memory and synaptic disruption.

Several studies proposed that Akt and ERK1/2 are involved in Aβ toxicity both in animal models [26] and hippocampal slices [27,36]. Our results showed that, along with increased memory loss, oxidative stress and caspase-9 activity, Aβ increased pAkt. Consistent with our results, some studies indicated that Akt phosphorylation (activation) is increased in AD; in particular, it has been shown that the level of pAkt is increased in the frontal cortices of AD patients and its amount is positively related to the severity of the pathology [37]. On the other hand, some other studies showed the decrement of Akt activity in animal and cellular AD models. For instance, Ghasemi et al. demonstrated that the amount of pAkt was decreased in primary hippocampal cell culture after $A\beta_{25-35}$ treatment [38]. Similarly, Cuie et al. have shown that pAkt is decreased in the APP/PS1 model of AD [39]. One of the most important targets of Akt is glycogen synthase kinase-3β (GSK3β), that is inhibited by the phosphorylation of its Ser9 residue [40]. GSK3 is highly expressed in the brain and has been identified as the principal kinase responsible for the hyperphosphorylation of tau in AD [41,42]. Several findings suggested that GSK3 activity might be increased in AD; however, direct evidence for this is still limited at present and some studies found no change in GSK3 activity [43] or reduced GSK3 activity [44] in AD. In our model, the enhancement of Akt activity leads to GSK3β inhibitory phosphorylation. Currently, we do not know if the activation of this pathway takes part in the pro-apoptotic effect induced by AβO i.c.v. injection, or represents a survival-oriented response that eventually proves abortive. In line with our findings, Jimenez et al. [45] demonstrated that the PI3K/Akt/GSK3β signaling pathway is directly impacted by Aβ exposure and in a $PS1_X$APP tg model at an early stage, despite the Aβ plaques, the prosurvival PI3K/Akt/GSK3β pathway is activated.

ERK1/2 are two similar kinases of the MAPK family which modulate a series of shared functions. Accumulating evidence is available showing that ERK1/2 is involved in different aspects of AD pathology [46]. However, there is an evident controversy about ERK1/2; while some studies elucidated that Aβ inhibits ERK1/2 and the restoring ERK1/2 activity is protective against Aβ-related toxicity [47,48], some other experiments showed that Aβ has no effect on ERK 1/2 activity [49] and yet others demonstrated that Aβ-induced cell death is concomitant with increased levels of ERK1/2 [26,50]. In the present study, $A\beta_{1-42}O$-induced memory impairment and apoptosis are accompanied by increased levels of ERK1/2 phosphorylation both in the hippocampus and cerebral cortex. Thus, it might be suggested that PI3K/Akt/GSK3β and MAPK/ERK1/2 pathways are involved in $A\beta_{1-42}O$-related toxicity in our experimental model.

5. Conclusions

In conclusion, our study demonstarted that a single i.c.v. injection of $A\beta_{1-42}O$ resulted in a significant impairment of memory function, imbalances in the redox status, apoptotic cell death and synaptic dysfunction. The i.c.v. administration of Aβ peptides into

the mice brain is a valid model of early AD. At present, there are a number of very valuable tools to study AD, but we should not forget that they are just models with their intrinsic limitations. For instance, transgenic models mostly reflect genetic forms of the disease, but AD is primarily a sporadic disorder, this can be partially mimicked by injections of Aβ into the rodent brain. Acute models unfortunately do not reproduce the gradual rise in Aβ occurring over many years in humans and it is unlikely that they reproduce the chronic AD phenotype. We must also admit that, in addition to providing only a partial model of AD, the invasive nature of Aβ infusion inevitably brings about brain injury, which may contribute to the induction of inflammation observed in these models. However, the use of acute injections may help to better understand how Aβ impairs specific signaling pathways leading to synaptic and memory dysfunctions, and this is crucial when designing new therapeutic strategies. It is also important to note that our model produces cognitive deficits much faster than transgenic animal models, in which memory impairments mostly develop within months.

In conclusion, our model seems to be promising as an early "filter" to evaluate the neuroprotective potential of compounds targeting Aβ or its downstream pathways observed in early AD. In particular, the involvement of PI3 K/Akt/GSK3β and MAPK/ERK1/2 pathways in Aβ toxicity suggests a therapeutic target for the treatment of neurodegenerative disorders, such as AD, in which apoptosis and oxidative stress play a relevant role.

Conflict of interest statement

The authors declare that there are no conflicts of interest.

Acknowledgments

This work was supported by Ministero dell'Istruzione, dell'Università e della Ricerca (MIUR), FIRB Accordi di programma 2011 (project: RBAP11HSZS), PRIN 2010 (project: 2010PWNJXK_002) and Fondazione del Monte di Bologna e Ravenna.

References

[1] J Hardy, D J Selkoe, The amyloid hypothesis of Alzheimer's disease: progress and problems on the road to therapeutics, Science 297 (2002) 353–356, http://dx doi org/10 1126/science 1072994

[2] K N Dahlgren, A M Manelli, W B J Stine, L K Baker, G A Krafft, M J LaDu, Oligomeric and fibrillar species of amyloid-beta peptides differentially affect neuronal viability, J Biol Chem 277 (2002) 32046–32053, http://dx doi org/10 1074/jbc M201750200

[3] C Haass, D J Selkoe, Soluble protein oligomers in neurodegeneration: lessons from the Alzheimer's amyloid beta-peptide, Nat Rev Mol Cell Biol 8 (2007) 101–112, http://dx doi org/10 1038/nrm2101

[4] C A McLean, R A Cherny, F W Fraser, S J Fuller, M J Smith, K Beyreuther, et al , Soluble pool of Abeta amyloid as a determinant of severity of neurodegeneration in Alzheimer's disease, Ann Neurol 46 (1999) 860–866, http://dx doi org/10 1002/1531-8249(199912)46:6<860:AID-ANA8>3 0 CO;2-M

[5] A M Fagan, M A Mintun, R H Mach, S Y Lee, C S Dence, A R Shah, et al , Inverse relation between in vivo amyloid imaging load and cerebrospinal fluid Abeta42 in humans, Ann Neurol 59 (2006) 512–519, http://dx doi org/10 1002/ana 20730

[6] C Chambon, N Wegener, A Gravius, W Danysz, Behavioural and cellular effects of exogenous amyloid-β peptides in rodents, Behav Brain Res 225 (2011) 623–641, http://dx doi org/10 1016/j bbr 2011 08 024

[7] D Puzzo, W Gulisano, A Palmeri, O Arancio, Rodent models for Alzheimer's disease drug discovery, Expert Opin Drug Discov 10 (2015) 703–711, http://dx doi org/10 1517/17460441 2015 1041913

[8] F M LaFerla, S Oddo, Alzheimer's disease: abeta, tau and synaptic dysfunction, Trends Mol Med 11 (2005) 170–176, http://dx doi org/10 1016/j molmed 2005 02 009

[9] K Herrup, Reimagining alzheimer's Disease?An age-Based hypothesis, J Neurosci 30 (2010) 16755–16762, http://dx doi org/10 1523/JNEUROSCI 4521-10 2010

[10] E Radi, P Formichi, C Battisti, A Federico, Apoptosis and oxidative stress in neurodegenerative diseases, J Alzheimers Dis 42 (2014) S125–S152, http://dx doi org/10 3233/JAD-132738

[11] D L Marcus, C Thomas, C Rodriguez, K Simberkoff, J S Tsai, J A Strafaci, et al , Increased peroxidation and reduced antioxidant enzyme activity in alzheimer's disease, Exp Neurol 150 (1998) 40–44 http://www ncbi nlm nih gov/pubmed/9514828

[12] M Padurariu, A Ciobica, L Hritcu, B Stoica, W Bild, C Stefanescu, Changes of some oxidative stress markers in the serum of patients with mild cognitive impairment and Alzheimer's disease, Neurosci Lett 469 (2010) 6–10, http://dx doi org/10 1016/j neulet 2009 11 033

[13] M A Ansari, S W Scheff, Oxidative stress in the progression of Alzheimer disease in the frontal cortex, J Neuropathol Exp Neurol 69 (2010) 155–167, http://dx doi org/10 1097/NEN 0b013e3181cb5af4

[14] M Obulesu, M J Lakshmi, Apoptosis in alzheimer's disease: an understanding of the physiology, pathology and therapeutic avenues, Neurochem Res 39 (2014) 2301–2312, http://dx doi org/10 1007/s11064-014-1454-4

[15] C W Cotman, Apoptosis decision cascades and neuronal degeneration in alzheimer's disease, Neurobiol Aging 19 (1998) S29–S32 http://www ncbi nlm nih gov/pubmed/9562464

[16] K Frebel, S Wiese, Signalling molecules essential for neuronal survival and differentiation, Biochem Soc Trans 34 (2006) 1287–1290, http://dx doi org/10 1042/BST0341287

[17] S Mondragòn-Rodriguez, G Perry, X Zhu, P I Moreira, S Williams, Glycogen synthase kinase 3: A point of integration in alzheimer's disease and a therapeutic target? Int J Alzheimers Dis 2012 (2012), http://dx doi org/10 1155/2012/276803

[18] A Tarozzi, A Merlicco, F Morroni, F Franco, G Cantelli-Forti, G Teti, et al , Cyanidin 3-O-glucopyranoside protects and rescues SH-SY5Y cells against amyloid-beta peptide-induced toxicity, Neuroreport 19 (2008) 1483–1486, http://dx doi org/10 1097/WNR 0b013e32830fe4b8

[19] H S Hong, I Maezawa, N Yao, B Xu, R Diaz-Avalos, S Rana, et al , Combining the rapid MTT formazan exocytosis assay and the MC65 protection assay led to the discovery of carbazole analogs as small molecule inhibitors of Abeta oligomer-induced cytotoxicity, Brain Res 1130 (2007) 223–234, http://dx doi org/10 1016/j brainres 2006 10 093

[20] I Maezawa, H S Hong, R Liu, C Y Wu, R H Cheng, M P Kung, et al , Congo red and thioflavin-T analogs detect Abeta oligomers, J Neurochem 104 (2008) 457–468, http://dx doi org/10 1111/j 1471-4159 2007 04972 x

[21] V Gupta, K Rao, Anti-amyloidogenic activity of S-allyl-L-cysteine and its activity to destabilize Alzheimer's beta-amyloid fibrils in vitro, Neurosci Lett 429 (2007) 75–80 http://www ncbi nlm nih gov/pubmed/18023978

[22] A Ennaceur, J Delacour, A new one-trial test for neurobiological studies of memory in rats 1: Behavioral data, Behav Brain Res 31 (1988) 47–59 http://www ncbi nlm nih gov/pubmed/3228475

[23] F Morroni, G Sita, A Tarozzi, G Cantelli-Forti, P Hrelia, Neuroprotection by 6-(methylsulfinyl)hexyl isothiocyanate in a 6-hydroxydopamine mouse model of Parkinson's disease, Brain Res 1589 (2014) 93–104, http://dx doi org/10 1016/j brainres 2014 09 033

[24] F Morroni, A Tarozzi, G Sita, C Bolondi, J M Zolezzi Moraga, G Cantelli-Forti, et al , Neuroprotective effect of sulforaphane in 6-hydroxydopamine-lesioned mouse model of Parkinson's disease, Neurotoxicology 36 (2013) 63–71, http://dx doi org/10 1016/j neuro 2013 03 004

[25] V A Movsesyan, A G Yakovlev, E A Dabaghyan, B A Stoica, A I Faden, Ceramide induces neuronal apoptosis through the caspase-9/caspase-3 pathway, Biochem Biophys Res Commun 299 (2002) 201–207, http://dx doi org/10 1016/S0006-291X(02)02593-7

[26] R Ghasemi, A Zarifkar, K Rastegar, N Maghsoudi, M Moosavi, Insulin protects against Aβ-induced spatial memory impairment, hippocampal apoptosis and MAPKs signaling disruption, Neuropharmacology 85 (2014) 113–120, http://dx doi org/10 1016/j neuropharm 2014 01 036

[27] M Nassif, J Hoppe, K Santin, R Frozza, L L Zamin, F Simão, et al , Beta-Amyloid peptide toxicity in organotypic hippocampal slice culture involves Akt/PKB, GSK-3beta, and PTEN, Neurochem Int 50 (2007) 229–235, http://dx doi org/10 1016/j neuint 2006 08 008

[28] M Stanciu, Y Wang, R Kentor, N Burke, S Watkins, G Kress, et al , Persistent activation of ERK contributes to glutamate-induced oxidative toxicity in a neuronal cell line and primary cortical neuron cultures, J Biol Chem 275 (2000) 12200–12206, http://dx doi org/10 1074/jbc 275 16 12200

[29] J J Palop, L Mucke, Amyloid-beta-induced neuronal dysfunction in Alzheimer's disease: from synapses toward neural networks, Nat Neurosci 13 (2010) 812–818, http://dx doi org/10 1038/nn 2583

[30] J H Jhoo, H C Kim, T Nabeshima, K Yamada, E J Shin, W K Jhoo, et al , beta-Amyloid (1–42)-induced learning and memory deficits in mice: involvement of oxidative burdens in the hippocampus and cerebral cortex, Behav Brain Res 155 (2004) 185–196, http://dx doi org/10 1016/j bbr 2004 04 012

[31] F Cetin, S Dincer, The effect of intrahippocampal beta amyloid (1–42) peptide injection on oxidant and antioxidant status in rat brain, Ann N Y Acad Sci 1100 (2007) 510–517, http://dx doi org/10 1196/annals 1395 056

[32] D A Kubli, A Gustafsson, Mitochondria and mitophagy: the yin and yang of cell death control, Circ Res 111 (2012) 1208–1221, http://dx doi org/10 1161/CIRCRESAHA 112 265819
[33] J a Keeble, A P Gilmore, Apoptosis commitment-translating survival signals into decisions on mitochondria, Cell Res 17 (2007) 976–984, http://dx doi org/10 1038/cr 2007 101
[34] A Tarozzi, F Morroni, A Merlicco, C Bolondi, G Teti, M Falconi, et al , Neuroprotective effects of cyanidin 3-O-glucopyranoside on amyloid beta (25–35) oligomer-induced toxicity, Neurosci Lett 473 (2010) 72–76, http:// dx doi org/10 1016/j neulet 2010 02 006
[35] A Tarozzi, A Merlicco, F Morroni, C Bolondi, P Di Iorio, R Ciccarelli, et al , Guanosine protects human neuroblastoma cells from oxidative stress and toxicity induced by Amyloid-beta peptide oligomers, J Biol Regul Homeost Agents 24 (2010) 297–306 http://www ncbi nlm nih gov/pubmed/20846477
[36] Y Chong, Y Shin, E Lee, R Kayed, C G Glabe, A J Tenner, ERK1/2 activation mediates Abeta oligomer-induced neurotoxicity via caspase-3 activation and tau cleavage in rat organotypic hippocampal slice cultures, J Biol Chem 281 (2006) 20315–20325, http://dx doi org/10 1074/jbc M601016200
[37] A Rickle, N Bogdanovic, I Volkman, B Winblad, R Ravid, R Cowburn, Akt activity in Alzheimer's disease and other neurodegenerative disorders, Neuroreport 15 (2004) 955–959 http://www ncbi nlm nih gov/pubmed/ 15076714
[38] R Ghasemi, M Moosavi, A Zarifkar, K Rastegar, N Maghsoudi, The interplay of akt and ERK in Aβ toxicity and insulin-Mediated protection in primary hippocampal cell culture, J Mol Neurosci 57 (2015) 325–334, http://dx doi org/10 1007/s12031-015-0622-6
[39] W Cui, J Tao, Z Wang, M Ren, Y Zhang, Y Sun, et al , Neuregulin1beta1 antagonizes apoptosis via ErbB4-dependent activation of PI3-Kinase/Akt in APP/PS1 transgenic mice, Neurochem Res 38 (2013) 2237–2246, http://dx doi org/10 1007/s11064-013-1131-z
[40] D P Brazil, B A Hemmings, Ten years of protein kinase B signalling: a hard Akt to follow, Trends Biochem Sci 26 (2001) 657–664, http://dx doi org/10 1016/ S0968-0004(01)01958-2
[41] D B Flaherty, J P Soria, H G Tomasiewicz, J G Wood, Phosphorylation of human tau protein by microtubule-associated kinases: GSK3beta and cdk5 are key participants, J Neurosci Res 62 (2000) 463–472 http://www ncbi nlm nih gov/pubmed/11054815
[42] C Hooper, R Killick, S Lovestone, The GSK3 hypothesis of alzheimer's disease, J Neurochem 104 (2008) 1433–1439, http://dx doi org/10 1111/j 1471-4159 2007 05194 x
[43] J Pei, T Tanaka, Y Tung, E Braak, K Iqbal, I Grundke-Iqbal, Distribution levels, and activity of glycogen synthase kinase-3 in the Alzheimer disease brain, J Neuropathol Exp Neurol 56 (1997) 70–78
[44] J E Swatton, L A Sellers, R L Faull, A Holland, S Iritani, S Bahn, Increased MAP kinase activity in Alzheimer ' s and Down syndrome but not in schizophrenia human brain, Eur J Neurosci 19 (2004) 2711–2719, http://dx doi org/10 1111/j 1460-9568 2004 03365 x
[45] S Jimenez, M Torres, M Vizuete, R Sanchez-Varo, E Sanchez-Mejias, L Trujillo-Estrada, et al , Age-dependent accumulation of soluble amyloid beta (Abeta) oligomers reverses the neuroprotective effect of soluble amyloid precursor protein-alpha (sAPP(alpha)) by modulating phosphatidylinositol 3-kinase (PI3K)/Akt-GSK- 3beta pathway in Alzheimer mouse, J Biol Chem 286 (2011) 18414–18425, http://dx doi org/10 1074/jbc M110 209718
[46] X Zhu, H -G Lee, A K Raina, G Perry, M A Smith, The role of mitogen-Activated protein kinase pathways in alzheimer's disease, Neurosignals 11 (2002) 270–281 http://www ncbi nlm nih gov/pubmed/ 12566928
[47] M Townsend, T Mehta, D J Selkoe, Soluble Abeta inhibits specific signal transduction cascades common to the insulin receptor pathway, J Biol Chem 282 (2007) 33305–33312, http://dx doi org/10 1074/jbc M610390200
[48] M Y Liu, S Wang, W F Yao, Z J Zhang, X Zhong, L Sha, et al , Memantine improves spatial learning and memory impairments by regulating NGF signaling in APP/PS1 transgenic mice, Neuroscience 273 (2014) 141–151, http://dx doi org/10 1016/j neuroscience 2014 05 011
[49] M J Savage, Y G Lin, J R Ciallella, D G Flood, R W Scott, Activation of c-Jun N-Terminal kinase and p38 in an alzheimer's disease model is associated with amyloid deposition, J Neurosci 22 (2002) 3376–3385 (20026352 r22/9/3376)
[50] G Frasca, V Carbonaro, S Merlo, A Copani, M A Sortino, Integrins mediate beta-amyloid-induced cell-cycle activation and neuronal death, J Neurosci Res 86 (2008) 350–355, http://dx doi org/10 1002/jnr 21487